Metamaterial-Based Two Element MIMO Array Design for Wireless Portable Devices

Iftikhar ud Din[1], Arif Ullah[2], Daud Khan[3], Sarosh Ahmad[1], Muhammad Ali Babar Abbasi[2], and Tayeb A. Denidni[1]

[1]Centre Énergie Matériaux Télécommun. Inst. National de la Recherche Sci. (EMT-INRS) Montréal, QC G1K 9A9, Canada.
[2]Centre for Wireless Innovations (CWI), School of Electronics, Electrical Engineering and Computer Science (EEECS), Queen's University Belfast, BT7 1NN United Kingdom (UK).
[3]Department of Information and Communication Engineering, Chosun University, Gwangju, 61452, Republic of Korea.
Email: [1]{iftikhar.ud-din, sarosh.ahmad, tayeb.denidni}@inrs.ca, [2]{a.ullah, m.abbasi}@qub.ac.uk, [3]daudkhalil700@chosun.kr.

***Abstract*—In this work, we present a metamaterial-based approach to enhance isolation in a dual-element circular patch multiple-input multiple-output (MIMO) antenna operating at 5.5 GHz. The proposed metamaterial unit cell has a compact size of 4×5.8 mm^2 and is designed on a low-cost FR-4 substrate with a height of 1.6 mm. In MIMO configuration, two radiating elements separated by 10 mm exhibit an isolation level of 19.7 dB. To mitigate inter-element coupling, an eight-cell metamaterial slab is printed between patch elements, improving isolation to 24.3 dB by suppressing waves and minimizing near-field coupling. The antenna is excited via a conventional microstrip feed, which is subsequently modified to a stepped feed structure to achieve frequency reconfiguration. However, this shifts the resonant frequency to 5.7 GHz, achieving compatibility with WLAN bands. The performance of the proposed MIMO antenna is evaluated and the simulation results demonstrate a low envelope correlation coefficient, improved gain, and suppression of mutual coupling. Due to these attributes, the proposed design demonstrates suitability for wireless portable devices.**

***Index Terms*—Antenna design, metamaterial, MIMO antenna, mutual coupling, portable devices, S-parameters, WLAN.**

I. Introduction

Rapid progress in wireless communication has led to the emergence of fifth-generation (5G) networks, which play a transformative role in mobile and Internet of Things (IoT) technologies. These systems are designed to meet the ever-increasing demand for ultra-fast data transmission, enhanced security, improved capacity, and reduced latency [1]. The 5G spectrum is divided into three primary frequency ranges: low-band (up to 1GHz), mid-band (below and up to 6GHz, referred to as sub-6 GHz), and high-band (millimeter-wave spectrum) [2]. Among these, the sub-6 GHz frequency bands, especially n77 and n79, are widely adopted for commercial and industrial 5G deployments [3], while the 7.125 to 8.4 GHz band is a candidate for the 6G. A crucial component of 5G networks is the multiple-input multiple-output (MIMO) technology, which provides reliable and high-performance wireless connectivity [4]. Unlike traditional single-antenna configurations, MIMO employs multiple radiating elements positioned on a common substrate and arranged in specific geometries, such as orthogonal or parallel alignments, to operate within the same frequency range. This system leverages spatial multiplexing, a vital characteristic that enhances spectral efficiency and increases the number of users served simultaneously. Furthermore, MIMO enhances overall network performance by increasing data throughput, signal-to-noise ratio (SNR), and channel bandwidth, while effectively mitigating multipath fading, path loss, and atmospheric attenuation [5]. A MIMO antenna system includes multiple radiating elements, *w*here mutual coupling (MC) is a critical problem that requires critical attention. MC is usually unwanted because it disturbs the operation of the MIMO antenna. The interaction among the MIMO elements may deteriorate system performance by increasing MC, enhancing the envelope correlation coefficient (ECC), increasing channel capacity loss (CCL), reducing diversity gain (DG), and distorting radiation characteristics [6]. The main cause of this coupling is the placement of radiating elements in close proximity [6]. Various methods have been proposed for reducing the MC of MIMO elements. When numerous radiating elements are positioned adjacent to each other, the electric field produced by one element alters the current distribution on the other element. As a result, the radiation characteristics and input impedance of the MIMO antenna are influenced by the presence of the other elements. Since MC clearly deteriorates the performance of MIMO structures, the antenna elements that make up the array must be designed collectively as a single aperture with reduced MC.

To decrease the gap and MC between radiating elements, numerous techniques have been explored, such as defected ground structures (DGS), decoupling shapes, and metamaterial structures such as electromagnetic band gap (EBG) [6]. Metamaterial structures have attracted considerable attention in the past decade [7] due to their potential in manipulating electromagnetic waves to enhance antenna operation. They are widely used as shielding between two radiating antennas to minimize transmission and reduce electromagnetic interactions [6]. Some conceptual structures have also been reported to use metasurfaces as superstrates to minimize coupling among

This work is partially supported by the Department for the Economy of Northern Ireland under U.S. Ireland Research and Development Partnership under Grant USI 199.

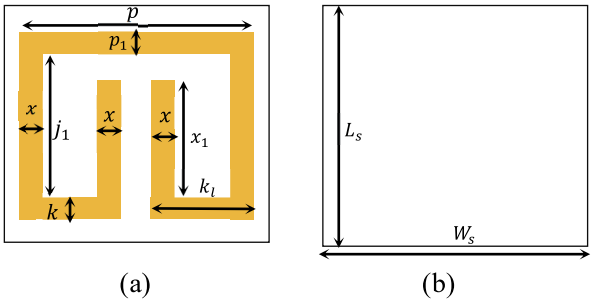

Fig. 1: Proposed unit cell: (a) Front view (b) Back view.

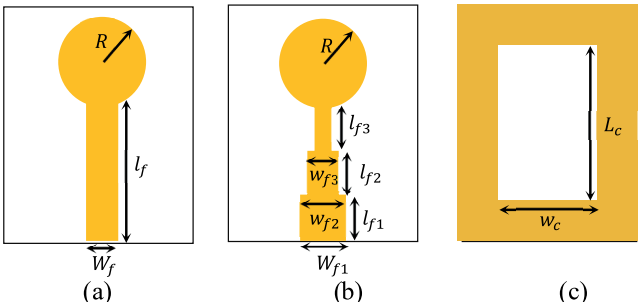

Fig. 2: Circular patch antenna: (a) Front view, (b) Front view with modified feed, and (c) Back view.

adjacent radiating elements [6]. Other techniques include the use of a shorting pin between two equally positioned antennas to reduce MC, or the use of four ground obstruction slots in an 8-element 5G MIMO antenna at sub-6GHz frequencies. Furthermore, tapered microstrip line and displacement line techniques have been reported to improve impedance matching of MIMO structures [8]. Designing MIMO antennas within this frequency range involves several critical challenges. The achievement of good isolation between radiating elements, maintaining a compact geometry suitable for portable and modern wireless devices, and simultaneously ensuring a wide impedance bandwidth and high gain remain the main design goals [9]. Several researchers have investigated MIMO antenna configurations operating around 5.8 GHz, focusing on compactness, isolation enhancement, and overall performance improvement. For example, a 2×2 microstrip MIMO antenna employing DGS was reported in [10], which improved isolation but resulted in a relatively large physical size. Likewise, a metamaterial-based dual-band MIMO antenna was presented in [11] to enhance gain performance, although its operational bandwidth was confined to narrow sub-bands in the 5 GHz spectrum. Previous studies have also used techniques such as EBG structures, parasitic resonators, and neutralization lines to effectively suppress MC between MIMO elements [12]. Although these designs can be effective, many come with increased manufacturing complexity or face challenges when miniaturized for use in portable devices. Some recent studies [13] have demonstrated compact designs with high isolation (greater than 20 dB). However, this often compromises either the antenna gain or its operational bandwidth. Moreover, very few approaches in the 5.8 GHz frequency band successfully achieve a balance among all critical performance factors, including minimal MC, high gain, small form factor, and straightforward fabrication.

In this paper, a metamaterial structure is proposed to decrease the MC between two circular patch antenna elements in the MIMO array. The design includes two circular patches fed by 50 Ω microstrip lines. The desired isolation is achieved by adding a 1×8 array of metamaterial unit cells between the two radiating elements. The resulting MIMO antenna exhibits a small MC ($|S_{21}|$ and $|S_{12}|$ lower than −20dB). The proposed MIMO antenna is a suitable candidate for several

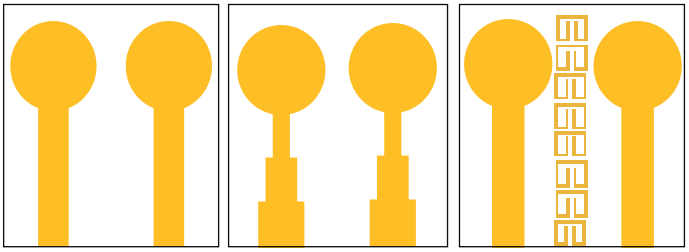

Fig. 3: Design modification of MIMO configuration: (a) MIMO with straight feed parallel configuration, (b) MIMO with steps feed parallel configuration, and (c) MIMO with straight feed parallel configuration with Metamaterial slab.

wireless applications due to its superior performance, in terms of lower ECC, higher DG, peak gain, and improved isolation. The remainder of this paper is organized as follows. Section II describes the step-by-step antenna design process within the simulation environment, Section II-A outlines the design and development of the proposed unit cell prototype, while Section II-B presents the development from a single element to a MIMO system. Section III presents the performance of the proposed MIMO antenna in terms of reflection and transmission coefficient, radiation patterns, ECC, and DG. Finally, Section IV concludes the paper by summarizing the key findings.

II. Design Methodology

The concepts of circular planar monopole antennas [14], split-ring resonator (SRR)-based structures [15], and stepped feed techniques for impedance matching [16] have been widely investigated and optimized in previous works. The proposed antenna is designed on a low-cost FR-4 substrate with overall dimensions of 20×35×1.6mm^3, a relative dielectric constant of $\varepsilon_r = 4.4$, and a loss tangent of $\tan\delta = 0.02$. The radiating element comprises two circular patches excited by a 50Ω microstrip feed line as depicted in Fig. 2 (a). To improve impedance matching, the feed line is segmented into three microstrip sections that provide a smooth transition, as illustrated in Fig. 2 (b). The stepped or segmented feed changes the operating frequency by modifying the current

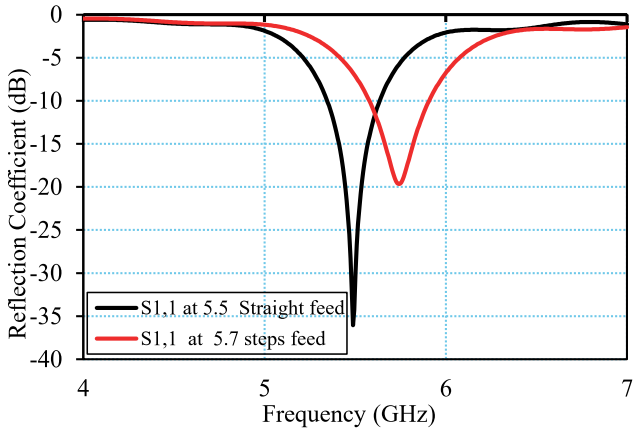

Fig. 4: Reflection coefficient of circular monopole antenna with straight and steps feed.

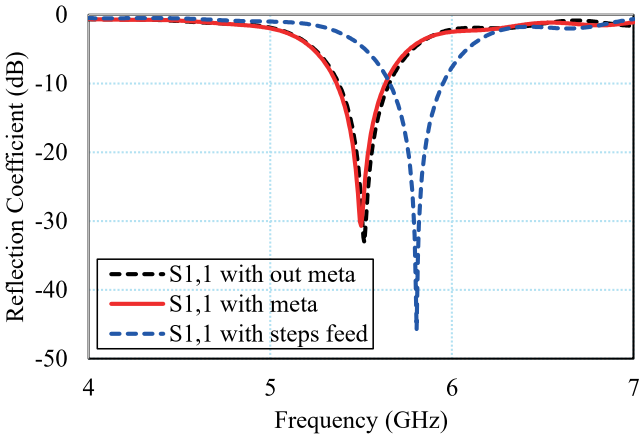

Fig. 6: Reflection coefficient of the proposed 2-element MIMO configuration with/without metamaterial and with steps feed.

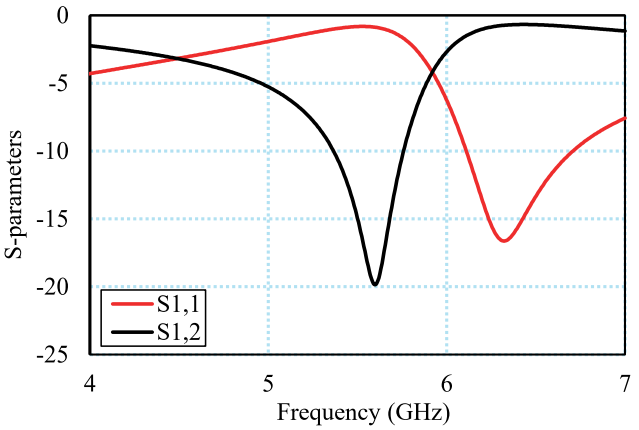

Fig. 5: S-parameters of the proposed metamaterial unit cell design.

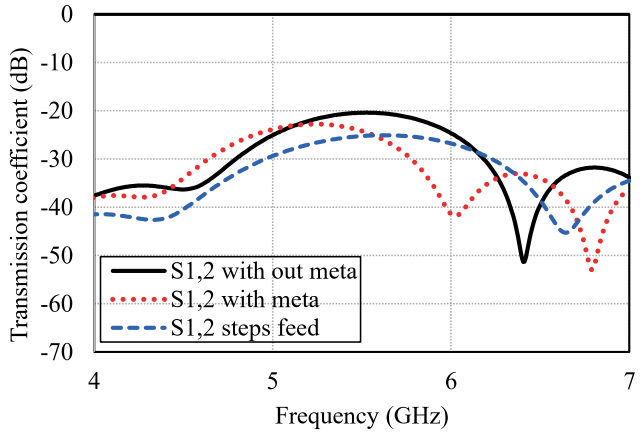

Fig. 7: Transmission coefficient of 2-element MIMO configuration with and without metamaterial and with stepped feed.

path and coupling with the antenna. By changing the step size, the antenna resonance shifts and achieves frequency reconfiguration without using active components. The corresponding ground-plane configuration of the proposed antenna is presented in Fig. 2 (c). The optimized design parameters of the circular patch MIMO and the metamaterial unit cell are w_c, W_g, L_s, W_s, l_f, W_f, R, L_c, p_1, p, j_1, x and x_1 whose values are 20, 20, 35, 35, 15, 3, 7.2, 20, 0.5, 4.5, 3, 0.5, and 1.5 (all in mm), respectively. The antenna performance has been analyzed in terms of the S parameters, the realized gain, and the radiation patterns. For full-wave electromagnetic simulation, the CST microwave studio was used to evaluate the MIMO configuration. The magnitude of simulated reflection coefficient (S11) is shown in Fig. 4. The antenna with a uniform feed line is observed to exhibit a resonance at 5.5 GHz, whereas the stepped feed line structure shifts the resonance frequency to 5.7 GHz to achieve frequency reconfiguration.

A. Design of the Proposed Metamaterial Unit Cell

Split-ring resonators (SRRs) are composed of metallic rings with gaps, patterned onto a dielectric substrate, and operate as subwavelength LC resonators, where the resonance frequency is determined by the rings' inductance and capacitance [17]. SRR-based metamaterial slabs function as electromagnetic shields, reducing surface wave propagation and minimizing near-field interactions between closely spaced antenna elements. This leads to isolation enhancement, while maintaining antenna performance and avoiding the need for large element spacing [18]. The geometry of the proposed metamaterial unit cell is illustrated in Fig. 1. The unit cell structure is also designed on an FR-4 substrate with a thickness of 1.6 mm. The proposed unit cell is compact with an overall dimension of $4\times5.8\times1.6$ mm^3. The designed configuration exhibits a resonant response with a frequency ranging from 5.5 to 5.7 GHz. As it can be observed that the antenna initially exhibits sub-optimal performance. However, by integrating a metamaterial slab, the isolation between antenna elements

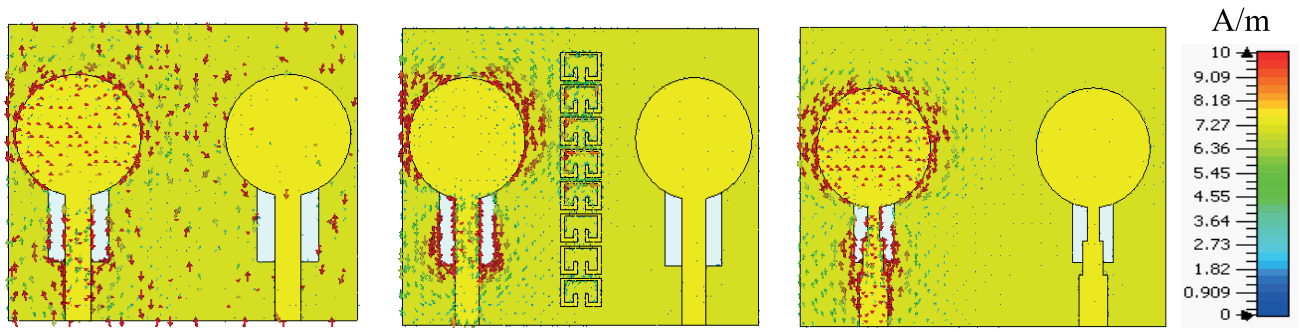

Fig. 8: Surface current distribution of an: (a) MIMO without metamaterial at 5.5 GHz, (b) MIMO with metamaterial at 5.5GHz, and (c) MIMO with stepped feed at 5.7 GHz.

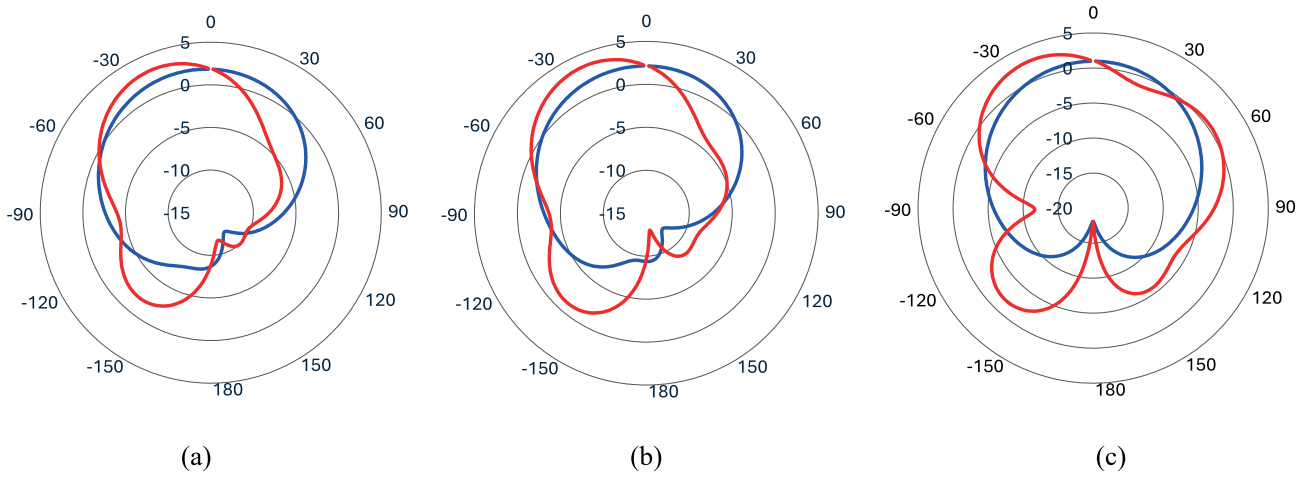

Fig. 9: Radiation pattern in E and H-plane, denoted by blue and red color, respectively: (a) without metamaterial at 5.5GHz (b) with metamaterial at 5.5GHz, and (c) with steps feed at 5.7GHz.

increased from 19.7 dB to 24.3 dB, while the realized gain showed a modest improvement. Moreover, these modifications mitigate the impact of mutual coupling and improve the overall radiation characteristics by addressing the primary limitations of the original design.

B. Development from Single Element to MIMO Configuration

Initially, a single circular monopole antenna was designed to operate efficiently. Subsequently, the feed line was modified, resulting in a shift in resonance frequency from 5.5 to 5.7 GHz, as shown in Fig. 2. In the second stage, an additional circular monopole antenna was placed adjacent to the first at a spacing of 10 mm, as illustrated in Fig. 3 (a). The second configuration, representing the modified-feed circular monopole MIMO antenna, is shown in Fig. 3 (b). Finally, to minimize MC, a metamaterial-based decoupling structure was introduced by placing an array of unit cells between the two circular monopole antennas to enhance isolation, as shown in Fig. 3 (c).

III. Simulation Results and Discussion

In this section, we present the performance of the proposed MIMO antenna design. The simulated reflection coefficient magnitude (S11) and the transmission coefficient magnitude (S21) for MIMO configurations, with/without metamaterial and with stepped feed, are presented in Fig. 6 and Fig. 7, respectively. The reflection coefficient for the MIMO antennas with and without metamaterial shows resonance at 5.5 GHz, while the stepped-feed MIMO configuration resonates at 5.7 GHz. For optimal MIMO performance, the MC must remain low to achieve good isolation. As shown in Fig. 7, the MIMO antenna that incorporates the metamaterial structure exhibits improved isolation of 24.3 dB compared to the configuration without metamaterial placement. Furthermore, the stepped-feed MIMO antenna also achieves isolation levels better than 20 dB, demonstrating the effectiveness of the proposed design.

The current distribution on the surface of the MIMO configuration at a certain frequency shows how the current couples from one radiating element to the adjacent radiating element

Table I: Comparison of the proposed design with reported MIMO antennas.

Ref	Size (mm^3)	Frequency (GHz)	BW (MHz)	Isolation (dB)	Peak Gain (dB)	ECC	DG
[19]	100×50×0.8	5.2–6.0	800	-25	6.57	0.032	9.83
[20]	40×40×0.8	3.4–3.6	200	-30	2.5	0.001	9.8
[21]	47.5×40×1.6	3.35–3.78	430	-15	3	<0.05	–
[22]	38.2×95.94×1.6	2.43–2.50	70	-24.67	7.08	0.0087	9.998
[23]	22.5×50×1.6	5.2–6.4	4000	-38	8.1	–	–
[24]	42.8×128.4×4.71	4–4.2	200	-37	7	–	–
This work	20×35×1.6	5.4–5.6, 5.6–5.8	200, 200	-24.3	3.7	<0.005	9.99

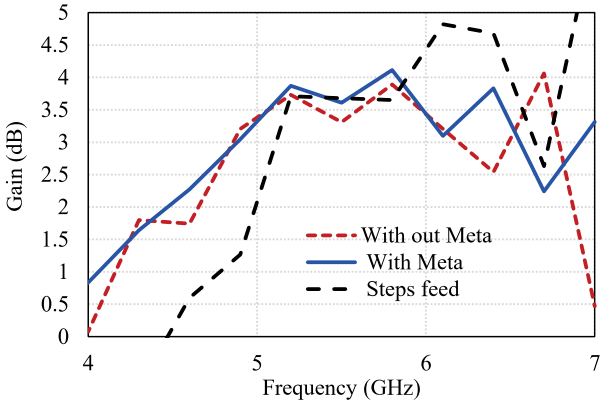

Fig. 10: Gain of the proposed two-element MIMO configuration with/without metamaterial and with stepped feed.

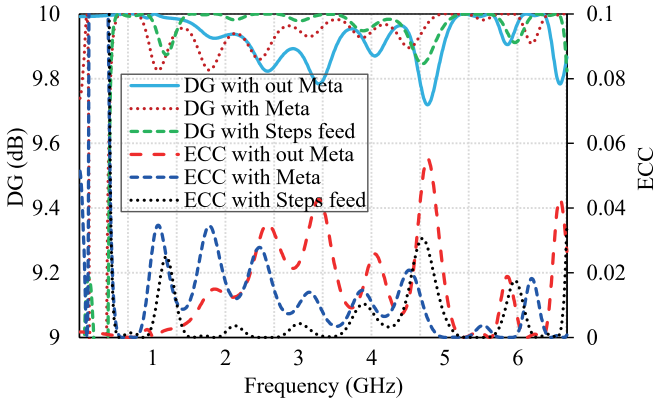

Fig. 11: Simulated DG and ECC of the proposed MIMO antenna with/without metamaterial and with steps feed.

and observes how one antenna is isolated from the other with respect to the current distribution. The surface current at 5.5 GHz for both the MIMO configuration with and without metamaterial is shown in Fig. 8. The two MIMO ports are excited, and the current from port 1 is distributed through the surface of the MIMO and coupled from one radiating element to another. Then, a metamaterial array of eight elements is placed in the middle of two radiating elements, and it can be observed in the figure that the presence of metamaterial leads to reduced coupling and improved isolation between antenna elements.

A. Diversity Performance

The radiation characteristics of MIMO antenna configurations, both with and without metamaterial structure, are investigated to evaluate performance enhancement. Fig. 9 presents the simulated radiation patterns at 5.5 GHz for both the E-plane ($\phi = 0°$) and ($\phi = 90°$) for the H-plane. As illustrated in the figure, the inclusion of the metamaterial introduces only a minor effect on the overall radiation direction, indicating that the metamaterial structure maintains stable radiation behavior while improving antenna isolation. Similarly, the simulated peak gains for both configurations are presented in Fig. 10. The MIMO antenna integrated with metamaterial unit cells exhibits an improved peak gain of 3.7 dB at 5.5 GHz, compared to 3.3 dB for the antenna without metamaterial. Furthermore, the stepped-feed antenna configuration demonstrates a slightly higher peak gain of 3.75 dB at 5.7 GHz.

B. Envelop Correlation Coefficient and Diversity Gain

The ECC is a parameter used to evaluate the individuality of the antennas, particularly where antennas are placed right next to each other, and is determined based on the radiation pattern. The ECC also takes into account the radiation pattern, polarization, and relative phase between two elements of a MIMO system and can be calculated as [25]. Similarly, DG refers to improvement in communication performance (typically in terms of signal reliability and reduced fading). From an antenna design perspective, it ensures low correlation, manages coupling, and provides distinct signal paths. DG can be mathematically expressed as [26].

$$\mathrm{DG} = 10\sqrt{1 - |\mathrm{ECC}|^2} \tag{1}$$

where the ECC is calculated using 2.

$$\mathrm{ECC} = \frac{\left|\iint_{4\pi} \mathbf{M}_i(\theta,\phi) \cdot \mathbf{M}_j(\theta,\phi)\, d\Omega\right|^2}{\iint_{4\pi} |\mathbf{M}_i(\theta,\phi)|^2\, d\Omega \iint_{4\pi} |\mathbf{M}_j(\theta,\phi)|^2\, d\Omega} \tag{2}$$

where $\mathbf{M}_i(\theta,\phi)$ and $\mathbf{M}_j(\theta,\phi)$ denote the radiation patterns when ports i and j are excited, respectively, and Ω represents the solid angle.

The calculated ECC and DG of the proposed MIMO array are presented in Fig. 11. As depicted in the figure, the ECC for antenna ports is very small and close to 0, which confirms a low correlation between the antennas, good isolation, and a higher DG. Furthermore, to highlight the significance and novelty of the proposed MIMO antenna design, we provide a detailed comparison of the design and different performance

metrics with the existing work in Table I. It can be observed that the proposed design is more compact in terms of size while targeting the desired frequency band with a bandwidth of 200 MHz. Moreover, isolation of 24.3 dB, a minimum ECC of 0.005, and a higher DG of 9.99 are achieved compared to the existing work while maintaining a peak gain of 3.7 dB.

IV. Conclusion

In this work, we investigated the impact of applying a metamaterial-based slab to reduce MC in the MIMO antenna system. Throughout the significance of the presented research, the structure, mock-up, and results concerning the MIMO antenna, suitable for MIMO utilization, have been thoroughly discussed. In this regard, we proposed a compact MIMO antenna design that operates at 5.5 GHz and is suitable for wireless portable devices. In the proposed design, it is observed that the modification in the feed leads to a resonance shift. Moreover, incorporating a metamaterial slab between the radiating elements of the MIMO antenna achieved excellent isolation between the antenna elements. The proposed antenna demonstrates superior performance, particularly in terms of ECC and DG, making it a strong candidate for practical MIMO applications. Future direction includes a metamaterial-embedded continuous aperture phased MIMO (CAP-MIMO) configuration using the same antenna structure and phase-controlling feed network.

References

[1] R. Li, Z. Mo, H. Sun, X. Sun, and G. Du, "A low-profile and high-isolated mimo antenna for 5G mobile terminal," *Micromachines*, vol. 11, no. 4, p. 360, 2020.

[2] M. J. Marcus, "5G and IMT for 2020 and beyond [spectrum policy and regulatory issues]," *IEEE Wireless Communications*, vol. 22, no. 4, pp. 2–3, 2015.

[3] S. S. Al-Bawri, M. T. Islam, M. J. Singh, E. Alyan, M. Jusoh, T. Sabapathy, S. Padmanathan, and K. Hossain, "Broadband sub-6GHz slot-based MIMO antenna for 5G nr bands mobile applications," in *Journal of Physics: Conference Series*, vol. 1962, no. 1. IOP Publishing, 2021, p. 012038.

[4] H. Zahra, W. A. Awan, W. A. E. Ali, N. Hussain, S. M. Abbas, and S. Mukhopadhyay, "A 28 GHz broadband helical inspired end-fire antenna and its mimo configuration for 5G pattern diversity applications," *Electronics*, vol. 10, no. 4, p. 405, 2021.

[5] A. K. Biswas and U. Chakraborty, "Reduced mutual coupling of compact MIMO antenna designed for WLAN and WiMAX applications," *International Journal of RF and Microwave Computer-Aided Engineering*, vol. 29, no. 3, p. e21629, 2019.

[6] M. Alibakhshikenari *et al.*, "A comprehensive survey on various decoupling mechanisms with focus on metamaterial and metasurface principles applicable to SAR and MIMO antenna systems," *IEEE Access*, vol. 8, pp. 192 965–193 004, 2020.

[7] A. A. Althuwayb, M. Alibakhshikenari, B. S. Virdee, N. Rashid, K. Kaaniche, A. B. Atitallah, A. Armghan, O. I. Elhamrawy, C. H. See, and F. Falcone, "Metasurface-inspired flexible wearable MIMO antenna array for wireless body area network applications and biomedical telemetry devices," *IEEE Access*, vol. 11, pp. 1039–1056, 2022.

[8] A. Iqbal, O. A Saraereh, A. Bouazizi, and A. Basir, "Metamaterial-based highly isolated MIMO antenna for portable wireless applications," *Electronics*, vol. 7, no. 10, p. 267, 2018.

[9] S. A. Ali, M. Wajid, A. Kumar, and M. S. Alam, "Design challenges and possible solutions for 5G SIW MIMO and phased array antennas: A review," *IEEE Access*, vol. 10, pp. 88 567–88 594, 2022.

[10] A. Kumar, A. Q. Ansari, B. K. Kanaujia, J. Kishor, and L. Matekovits, "A review on different techniques of mutual coupling reduction between elements of any MIMO antenna. Part 1: DGSs and parasitic structures," *Radio Science*, vol. 56, no. 3, pp. 1–25, 2021.

[11] D. Khan, A. Ahmad, and D.-Y. Choi, "Dual-band 5G MIMO antenna with enhanced coupling reduction using metamaterials," *Scientific Reports*, vol. 14, no. 1, p. 96, 2024.

[12] D. Pandurangan and N. Mishra, "Various mutual coupling reduction techniques for 5G: MIMO antenna," in *Microwave Devices and Circuits for Advanced Wireless Communication*. CRC Press, 2024, pp. 37–63.

[13] A. A. Megahed, M. Abdelazim, E. H. Abdelhay, and H. Y. Soliman, "Sub-6 GHz highly isolated wideband MIMO antenna arrays," *IEEE Access*, vol. 10, pp. 19 875–19 889, 2022.

[14] J. Liang, "Study of a circular disc monopole antenna for ultra wideband applications," *IEICE Proceeding Series*, vol. 12, pp. 81–84, 2004.

[15] J. B. Pendry, A. J. Holden, D. J. Robbins, and W. J. Stewart, "Magnetism from conductors and enhanced nonlinear phenomena," *IEEE transactions on microwave theory and techniques*, vol. 47, no. 11, pp. 2075–2084, 1999.

[16] G. Singh and U. Singh, "Triple-step feed line-based compact ultra-wideband antenna with quadruple band-notch characteristics," *International Journal of Electronics*, vol. 109, no. 2, pp. 271–292, 2022.

[17] M. Moniruzzaman, M. T. Islam, N. Misran, M. Samsuzzaman, T. Alam, and M. E. Chowdhury, "Inductively tuned modified split ring resonator based quad band epsilon negative (ENG) with near zero index (NZI) metamaterial for multiband antenna performance enhancement," *Scientific reports*, vol. 11, no. 1, p. 11950, 2021.

[18] T.-M. Jose Alfredo, J.-A. Hildeberto, F.-L. Ruben, R.-M. Arturo, P.-M. Angel, and G.-V. Ricardo, "Small-size eight-element MIMO metamaterial antenna with high isolation using modal significance method," *Sensors*, vol. 24, no. 19, p. 6266, 2024.

[19] M. Kaur and H. S. Singh, "Design and analysis of high isolated super compact 2× 2 MIMO antenna for WLAN application," *International Journal of RF and Microwave Computer-Aided Engineering*, vol. 31, no. 11, p. e22864, 2021.

[20] M. Anbarasu and J. Nithiyanantham, "Performance analysis of highly efficient two-port MIMO antenna for 5G wearable applications," *IETE Journal of Research*, vol. 69, no. 6, pp. 3594–3603, 2023.

[21] ——, "Performance analysis of highly efficient two-port MIMO antenna for 5G wearable applications," *IETE Journal of Research*, vol. 69, no. 6, pp. 3594–3603, 2023.

[22] K. Sharma and G. P. Pandey, "Two port compact MIMO antenna for ISM band applications," *Progress In Electromagnetics Research C*, vol. 100, pp. 173–185, 2020.

[23] I. Khan, Q. Wu, I. Ullah, S. U. Rahman, H. Ullah, and K. Zhang, "Designed circularly polarized two-port microstrip MIMO antenna for WLAN applications," *Applied Sciences*, vol. 12, no. 3, p. 1068, 2022.

[24] M. S. Sadiq, C. Ruan, H. Nawaz, M. A. B. Abbasi, and S. Nikolaou, "Mutual coupling reduction between finite spaced planar antenna elements using modified ground structure," *Electronics*, vol. 10, no. 1, p. 19, 2020.

[25] I. U. Din, S. Ullah, N. Mufti, R. Ullah, B. Kamal, and R. Ullah, "Metamaterial-based highly isolated MIMO antenna system for 5G smartphone application," *International Journal of Communication Systems*, vol. 36, no. 3, p. e5392, 2023.

[26] O. Khan, S. Khan, S. N. K. Marwat, N. Gohar, M. Bilal, and M. Dalarsson, "A novel densely packed 4× 4 MIMO antenna design for UWB wireless applications," *Sensors*, vol. 23, no. 21, p. 8888, 2023.